

The influence of papermaking process parameters on the performance of medical dialysis base paper and predictive study on indicator performance

K. J. Wang ^a, F. K. Kong ^a, W. T. Zhu ^a, J. Li ^{a,*}, L. Z. Sha ^a, J. B. Chen ^b

^a School of Environmental and Natural Resources, Zhejiang University of Science and Technology, Hangzhou, 310023, China

^b Winbon Schoeller New Materials Co., Ltd, Quzhou, 324400, China

This study explores the effects of paper making parameters (softwood pulp ratio, beating degrees) on medical dialysis base paper performance (air permeability, pore properties). Increasing softwood pulp ratio enhances air permeability via better pore connectivity, while higher beating degrees reduce it due to denser pore structure. A predictive model using linear path function (L₂) and pore connectivity index (S value) is developed. SEM and pore analysis validate the mechanism, emphasizing the balance for ISO 11607 compliance. Results support process optimization and performance prediction.

(Received June 13, 2025; Accepted September 11, 2025)

Keywords: Medical dialysis base paper, Papermaking process parameters, Air permeability, Fiber morphology, Pore connectivity, Linear path function

1. Introduction

Medical dialysis paper, as a medical packaging material, must exhibit both high air permeability and bacterial barrier properties, which are primarily determined by fiber network structure and pore characteristics. Existing research often focuses on the impact of single process parameters, while systematic analysis of multi-parameter synergistic regulation mechanisms, such as softwood/hardwood ratios and beating processes, remains limited. Additionally, traditional methods struggle to quantify pore connectivity, hindering the accuracy of performance prediction[1].

This study employs softwood and hardwood pulps as raw materials to systematically explore the effects of their ratios (1:0 to 5:5) and beating degrees (softwood: 20–36°SR; hardwood: 22–49°SR) on the air permeability, pore size distribution, and pore connectivity of medical dialysis base paper. The linear path function (L₂) and integral S-value are introduced to quantitatively characterize pore structures. Fiber morphology and pore structure correlations are revealed through MORFI fiber analysis, SEM, and air permeability testing. A process parameter-performance prediction model is established. The innovation lies in proposing a multi-scale pore connectivity quantification method, offering theoretical guidance for optimizing medical dialysis paper performance and industrial production

* Corresponding author: jingli@zust.edu.cn
<https://doi.org/10.15251/JOBM.2025.173.205>

2. Materials and methods

2.1. Experimental materials and chemicals

Raw materials and reagents are listed in Table 1.

Table 1. Experimental raw materials and reagents.

Name	Parameters	Manufacturer
Hardwood pulp board	/	Xianyang Tongda Light Industry Co.
Softwood pulp board	/	China Pulp and Paper Research Institute
Cationic polyacrylamide	/	Henan Dongwanyuan Water Purification Co.
AKD sizing agent	Solid content: 15 g/L	Ming xiang Chemical Technology Co.
Wet-strength agent	Solid content: 15 g/L	Ming xiang Chemical Technology Co.

2.2. Fiber pretreatment and beating process

Before the production process of the base paper for medical dialysis paper, pre-treatment of the purchased fiber pulp board is required. The steps are as follows:

(1) Weigh 500 g each of the softwood pulp board and hardwood pulp board in Table 2 - 1, and tear them into pieces of approximately 3 x 3 cm.

(2) Place the pulp board fragments in a 1 L beaker, add about 800 ml of distilled water, and soak for 24 hours to fully swell.

(3) Defibrate the swelled wood pulp using a fiber defibrator (3,000 r/min, 5 min).

(4) Put the defibrated wood pulp fibers into a sealed bag and place it in a constant - temperature refrigerator for later use.

(5) Select a certain amount of defibrated softwood pulp and use a PFI vertical refiner to make the beating degree of the defibrated softwood pulp reach $20 \pm 1^\circ\text{SR}$.

(6) Select a certain amount of swollen hardwood pulp, place it in a fiber defibrator (3,000 r/min, 5 min) for defibration, and use a PFI vertical refiner to make the beating degree of the defibrated hardwood pulp reach $22 \pm 1^\circ\text{SR}$.

(7) Repeat steps (5) and (6) to obtain softwood pulp with beating degrees of $20 \pm 1^\circ\text{SR}$, $24 \pm 1^\circ\text{SR}$, $28 \pm 1^\circ\text{SR}$, $33 \pm 1^\circ\text{SR}$, and $36 \pm 1^\circ\text{SR}$ respectively, and obtain hardwood pulp with beating degrees of $22 \pm 1^\circ\text{SR}$, $26 \pm 1^\circ\text{SR}$, $35 \pm 1^\circ\text{SR}$, and $49 \pm 1^\circ\text{SR}$ respectively.

(8) Weigh 2 ± 0.2 g of pulp, place it in a rapid dryer to dry automatically until all the moisture is evaporated to obtain its solid content. Repeat 3-5 times and select the average value as the solid content of the pulp at this beating degree.

(9) Repeat step (8) to test the solid content of the remaining pulps.

(10) Put the tested pulp into a sealed bag, balance the moisture for 24 hours, and place it in a constant-temperature refrigerator for later use

2.3. Paper sheet forming process

Weigh coniferous pulp and hardwood pulp with a total mass of absolutely dry pulp of 1.884 g. The ratios of coniferous pulp to hardwood pulp are 1:0, 9:1, 8:2, 7:3, 6:4, and 5:5 respectively. Put the weighed pulp into a fiber defibrator (3,000 r/min, 5 min) for defibration, then add 1 mL of cationic pregelatinized starch with a concentration of 0.1%. After sufficient stirring, add 1 mL of AKD sizing agent with a concentration of 3.0% and 1 mL of wet strength agent with a concentration of 2.0%. After full stirring, form paper with a basis weight of $60 \pm 2 \text{ g} \cdot \text{m}^{-2}$ using a laboratory standard paper forming machine. Treat the formed paper according to the TAPPI T402 standard at a constant temperature and humidity for 24 hours, and finally measure its physical properties and air permeability

2.4. Methods for characterizing fiber morphology and paper properties

Analyze the main characteristics of papermaking fibers based on the MORFI type fiber analyzer. The basic steps are as follows:

(1) Weigh 300 mg of absolutely dry pulp at different beating degrees after pretreatment in Section 2.2.3.1 respectively. After defibration with a fiber defibrator (3,000 r/min, 5 min), dilute with 2 L of distilled water.

(2) Weigh 200 ml of the diluted pulp, which is equivalent to 30 mg of absolutely dry pulp, pour it into a sample cup and dilute it to 1 L.

(3) Launch the analysis software of the MORFI type fiber analyzer, and the analysis will be carried out automatically.

(4) After the detection is completed, the fiber analyzer automatically imports the report, obtaining the performance data such as the length and width of the detected fibers

2.4.1. Standardized procedure for air permeability and pore size analysis

(1) Air permeability

Use the air permeability tester (TEXTTEST FX30000) to test the air permeability of the prepared base paper for medical dialysis paper. The measurement pressure is 200 Pa, and the measurement area each time is 20 cm². Select 10 different sampling locations on each piece of base paper for medical dialysis paper and take the average air permeability [2].

(2) Mean pore size, maximum pore size and most probable pore size

Use the pore size analyzer to test the mean pore size, maximum pore size and most probable pore size of the prepared base paper for medical dialysis paper. Use GP16 as the wetting liquid. Select 10 different sampling locations on each piece of base paper for medical dialysis paper, and take the average values of their mean pore size, maximum pore size and most probable pore size [3].

2.4.2. Scanning electron microscope (SEM) image acquisition and pore structure analysis

Cut the prepared base paper for medical dialysis paper into squares with a size of 1x1 cm, stick them on the double-sided carbon conductive adhesive tape, spray gold, and use a scanning electron microscope (Hitachi SU - 1510) to scan the surface with an accelerating voltage of 15 kv [4].

3. Theoretical model and analytical method

3.1. Theoretical basis and calculation method of linear path function (L₂)

The Linear Path Function (L₂) is a statistical function used to characterize the pore connectivity in binary porous medium structures [5]. It is defined as follows: Randomly select a line segment in a given direction on the image, calculate the probability that all pixels on this line segment are located in the pore phase [6], and take this probability as a function of the line segment length, namely L₂. The calculation process of L₂ is as follows: First, select multiple directions (such as horizontal, vertical, diagonal, etc.) in the binary image and randomly sample line segments of different lengths along these directions. For each line segment, count the cases where all the pixels it contains are located in the pore phase, and calculate the proportion of these cases to the total number of sampling times, so as to obtain the variation trend of L₂ with the line segment length. When the line segment length is short, the L₂ value is relatively large, indicating that the pore structure is relatively continuous in the short range; as the line segment length increases, L₂ gradually decreases until it tends to be stable, indicating that the long-range connectivity is hindered by the fiber phase, reducing the continuity of the pores. The linear correlation function is defined as the probability that two pixels separated by a distance of δ on the original paper image of medical dialysis paper, as well as the pixels between the two pixels, are all located in the pore phase [7]. As shown in Figure 1, considering the influence of pixel pairs and inter-pixel pairs on the function, the pore connectivity information of the original paper of medical dialysis paper can be counted. The formula is as follows (X):

$$\Lambda_2^{(i)}(\xi_1, \xi_2) = \langle X(\xi_1) X(\xi_1 + \delta) X(\xi_1 + 2\delta) \dots X(\xi_1 + v\delta) \rangle \quad (1)$$

In the formula, $\langle \rangle$ represents the expectation operator, where $i = 0, 1, 2, \dots, n$.

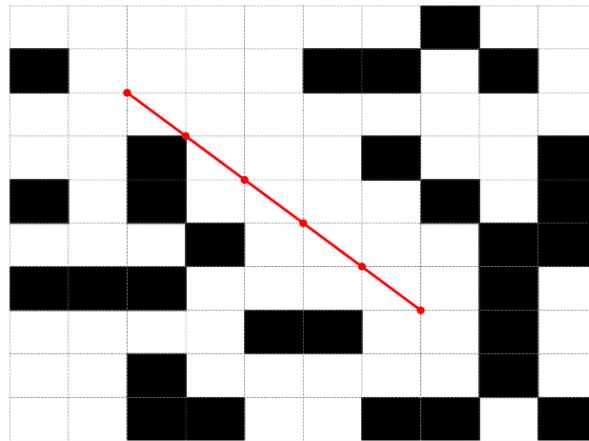


Fig 1. Schematic diagram of the linear path function.

3.2. Definition and physical meaning of the quantitative indicator (S Value) of pore connectivity

From a physical perspective, L_2 reflects the connectivity of pores at a specific scale, which is crucial for predicting the permeability of materials[8]. For example, in breathability research, the decline rate of L_2 can be used to characterize the complexity of the permeation paths of gases or liquid fluids in the medium[8]. By analyzing L_2 in different directions, the anisotropy of the pore structure can be evaluated, and then the fiber ratio, beating process or forming parameters can be optimized to achieve the desired pore characteristics of the material. Therefore, as an important statistical quantity for characterizing porous media, L_2 has extensive application value in materials science and engineering research.

To quantitatively characterize the connectivity comparison of L_2 , its integral value is adopted, as shown in (2):

$$\Sigma = \sum_{p=1}^{\theta} \Lambda_2(\rho) \quad (2)$$

The larger the S value, the better the overall pore connectivity. The smaller the S value, the worse the pore connectivity, with more paths being blocked.

4. Results and discussion

4.1. Fiber morphology test results

Table 2 shows the main characteristics of papermaking fibers obtained by the MORFI type fiber analyzer.

Table 2. Analysis results of MORFI type fiber analyzer.

Fiber Type	Number - average Length(mm)	Weight - average Length(mm)	Width (μm)	Coarseness (mg/m)	Aspect Ratio (Weight - average)
20 \pm 1°SR Coniferous Wood Pulp	1.312	2.061	34.3	0.0746	60.08746
24 \pm 1°SR Coniferous Wood Pulp	1.242	2.004	34.4	0.0826	58.25581
28 \pm 1°SR Coniferous Wood Pulp	1.218	1.883	32.2	0.0953	58.47826
33 \pm 1°SR Coniferous Wood Pulp	1.105	1.753	31.8	0.0830	55.12579
35 \pm 1°SR Coniferous Wood Pulp	1.035	1.736	34.7	0.0515	50.02882
22 \pm 1°SR Broad-leaved Wood Pulp	0.651	0.801	18.3	0.0207	43.77049
26 \pm 1°SR Broad-leaved Wood Pulp	0.667	0.780	16.1	0.0324	48.4472
35 \pm 1°SR Broad-leaved Wood Pulp	0.662	0.788	17.3	0.0258	45.54913
49 \pm 1°SR Broad-leaved Wood Pulp	0.637	0.739	16.5	0.0516	44.78788

In this study, the number-average length, weight-average length, width, and coarseness of fibers were measured using a MORFI-type fiber analyzer, and the aspect ratio based on the weight-average length was calculated. The experimental results showed that the number-average length of coniferous wood fibers ranged from 1.035 to 1.312 mm, while that of broad-leaved wood fibers ranged from 0.637 to 0.667 mm. These values are susceptible to the influence of short fibers. The weight-average length of coniferous wood fibers ranged from 1.736 to 2.061 mm, and that of broad-leaved wood fibers ranged from 0.739 to 0.801 mm. Compared with the fiber average length, which is easily affected by shorter fibers, the fiber weight-average length can better reflect the length characteristics of fibers.

In Table 2-2, the length, width, and coarseness of fibers can all affect the properties of the final paper sheet[9]. Among them, fiber length is the core morphological parameter affecting air permeability. Longer fibers (such as coniferous wood fibers) tend to form a three-dimensional network skeleton during the forming process. This structure can provide more through pores, thereby significantly improving air permeability[10] Long fibers improve pore connectivity and reduce the tortuosity of gas transmission, making air permeability nonlinearly positively correlated with fiber length[11] Short fibers (such as broad-leaved wood fibers or fragments generated during the beating process) tend to fill pores and increase the compactness of the fiber network, resulting in a decrease in air permeability. The presence of short fibers can block the pores formed by long fibers and increase the complexity of the gas transmission path[12].Fiber width mainly affects air permeability in the following ways: Wider fibers occupy more space during the forming process, resulting in a

lower porosity of the fiber network. However, wider fibers may also form larger pores, especially near the fiber intersection points. This effect may partially offset the decrease in porosity. Wider fibers have a larger contact area, which may enhance the bonding strength between fibers. However, at the same time, it also increases the compactness of the fiber network, thus having a dual impact on air permeability. Narrower fibers usually have higher flexibility and can better adapt to the topological structure of the fiber network during the forming process, forming a more uniform pore distribution, which is conducive to the improvement of air permeability. Fiber coarseness (mass per unit length) is a comprehensive parameter of fiber morphology. Its action mechanism includes the regulation of fiber stacking density, the trade-off of inter-fiber bonding strength, and the fluidity and forming uniformity of fibers[13] The length, width, and coarseness of fibers do not act independently but jointly regulate air permeability through complex coupling relationships. Longer fibers are more likely to form a high-porosity network structure when the width is smaller, while wider fibers may partially offset the disadvantage of shorter length by increasing pore size. Higher coarseness will significantly reduce air permeability when the fiber length is shorter, but when the fiber length is longer, its negative impact may be partially offset by the fiber skeleton effect.

4.2. Regulation rules of process parameters on air permeability

4.2.1. Regulation rules of coniferous wood pulp proportion on air permeability

In order to analyze the influence of the change in the proportion of coniferous wood pulp on the properties of the original paper for medical dialysis, the data obtained from the experiment were analyzed. Figure 2 shows the influence of the proportion of coniferous wood on the air permeability of the original paper for medical dialysis.

As shown in Figure 3, with the increase in the proportion of coniferous wood pulp, the air permeability of the original paper for medical dialysis shows an obvious upward trend. For example, when the beating degree of coniferous wood pulp is $20 \pm 1^\circ\text{SR}$ and that of broad-leaved wood pulp is $22 \pm 1^\circ\text{SR}$, as the proportion of coniferous wood pulp increases to 50%, 60%, 70%, 80%, 90%, and 100%, the air permeability of the original paper for medical dialysis rises to 58.36, 72.23, 93.76, 100.4, 113.04, and 172.14 L/(m²·s) respectively. Similarly, for coniferous wood pulps with beating degrees of $24 \pm 1^\circ\text{SR}$, $28 \pm 1^\circ\text{SR}$, $33 \pm 1^\circ\text{SR}$, and $36 \pm 1^\circ\text{SR}$, as well as broad-leaved wood pulps with beating degrees of $26 \pm 1^\circ\text{SR}$, $35 \pm 1^\circ\text{SR}$, and $49 \pm 1^\circ\text{SR}$, the overall trend shows an upward tendency. From the perspective of fiber morphology, this phenomenon may be related to the longer length and higher aspect ratio of coniferous wood pulp fibers. Coniferous wood pulp fibers have a significant length advantage (1.0-1.3 mm) and a relatively large aspect ratio (about 60:1). Compared with broad-leaved wood fibers (average 0.65-0.67 mm), they are more likely to form a three-dimensional network skeleton structure during the forming process. This topological structure forms a large number of through pores with low bending factors in the Z-direction dimension, providing an efficient path for gas transmission and thus enhancing air permeability[11] Further analysis shows that when the proportion of coniferous wood exceeds 70%, the slope of the air permeability increase significantly increases, which may be related to the breakthrough of the critical percolation threshold. At this time, the fiber network begins to form continuous permeable pathways. Therefore, it can be concluded that when coniferous wood fibers account for a high proportion, the paper structure will form a looser structure, thereby increasing air permeability. At the medical functional level, the results of this study are significantly associated with the ISO 11607 standard. Although high air permeability

is conducive to gas penetration, an excessively high porosity will lead to the deterioration of anti-bacterial performance[14] It is necessary to control the maximum pore size to be less than $35\ \mu\text{m}$ while ensuring air permeability to meet the antibacterial requirements.

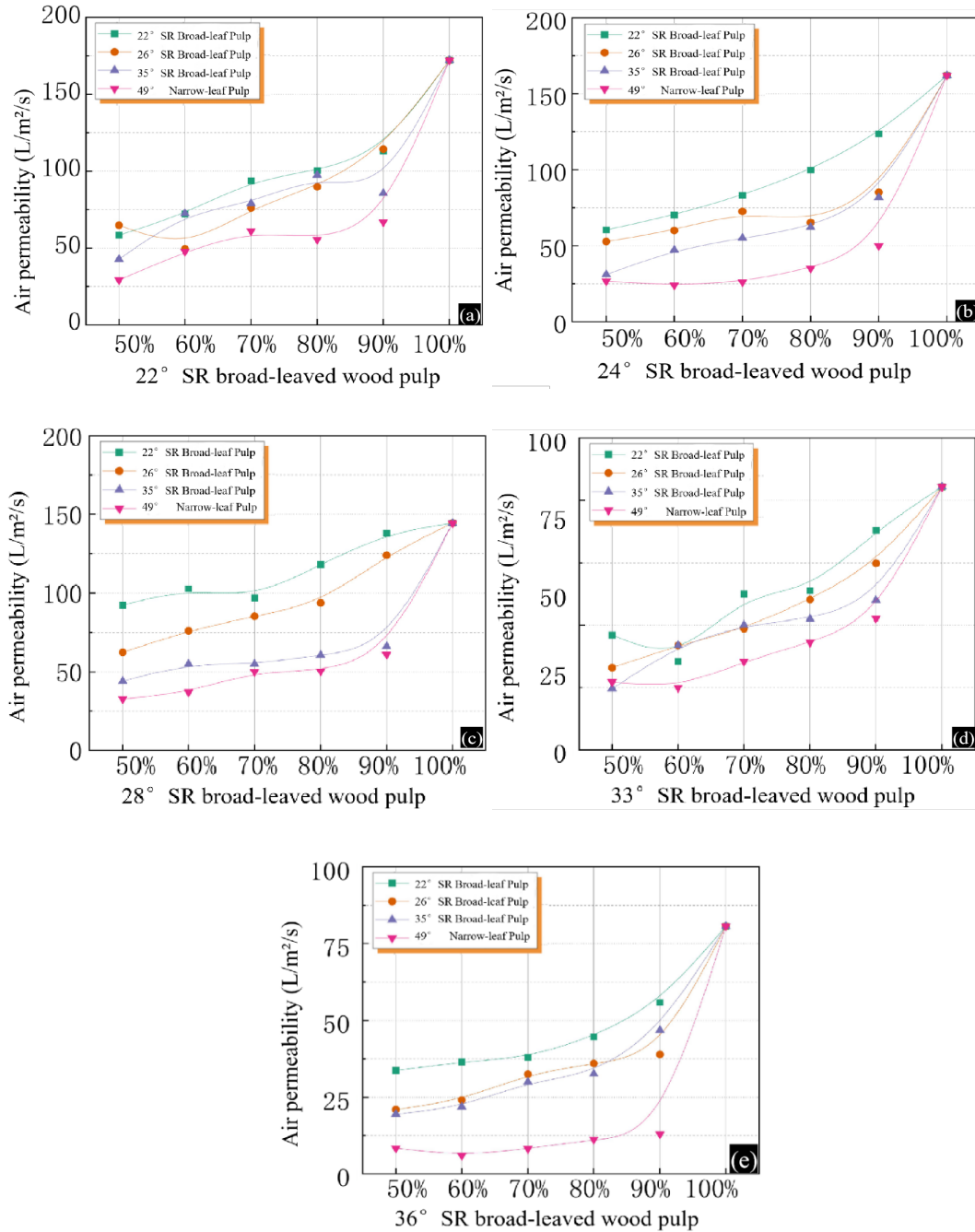


Fig. 2. The air permeability of the original paper for medical dialysis with different proportions of coniferous wood pulp under different beating degrees of coniferous wood pulp. (a) Coniferous wood pulp at $20\pm 1^\circ\text{SR}$ (b) Coniferous wood pulp at $24\pm 1^\circ\text{SR}$ (c) Coniferous wood pulp at $28\pm 1^\circ\text{SR}$ (d) Coniferous wood pulp at $33\pm 1^\circ\text{SR}$ (e) Coniferous wood pulp at $36\pm 1^\circ\text{SR}$.

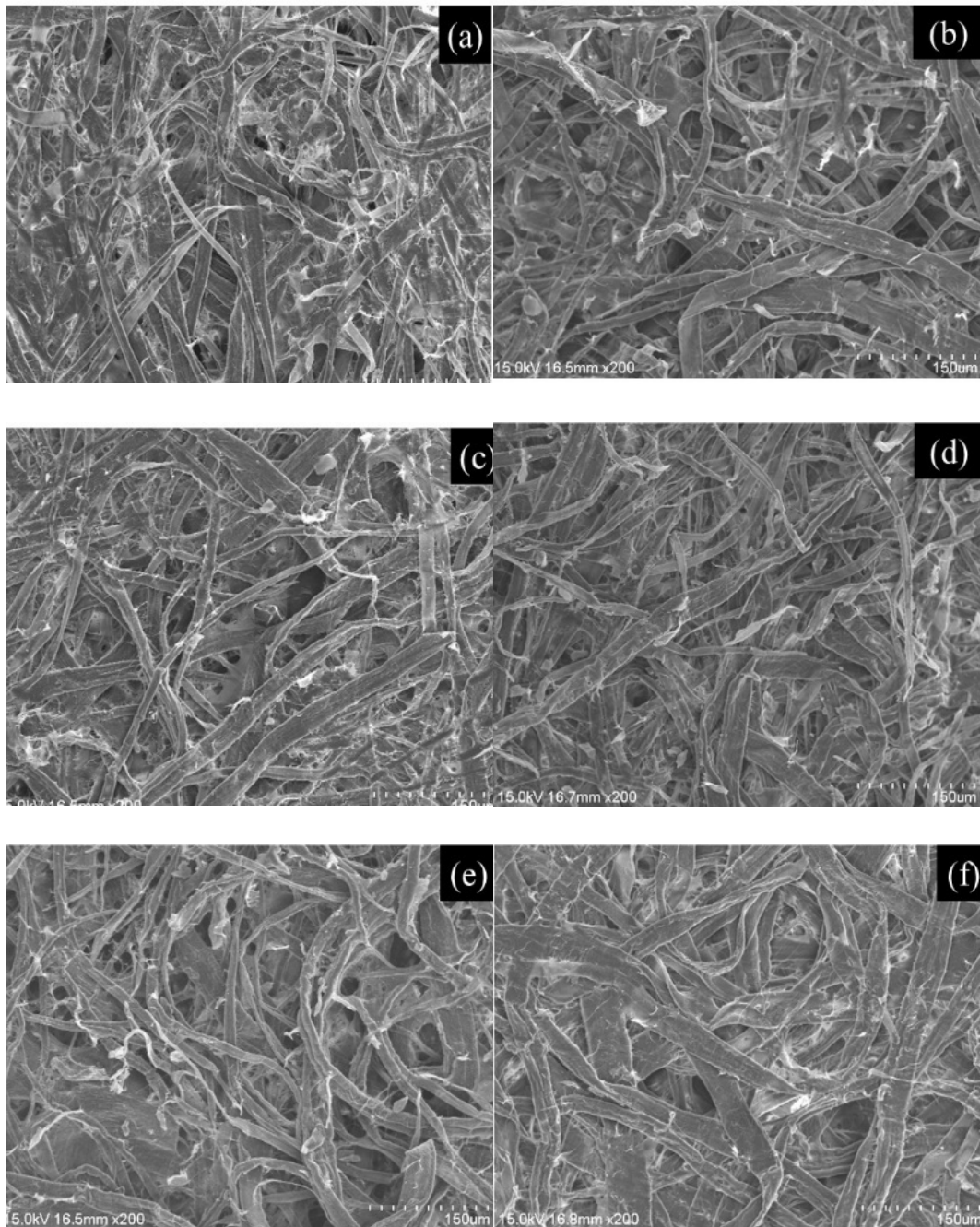


Fig. 3. SEM Images of the paper structure of the original medical dialysis paper under different proportions of coniferous wood pulp (a) 50%, (b) 60%, (c) 70%, (d) 80%, (e) 90%, (f) 100%.

To analyze the influence of the change in the proportion of coniferous wood pulp on the overall pore space of the original medical dialysis paper, Figures 3 a-f are SEM images taken when the beating degree of coniferous wood pulp is $20 \pm 1^\circ \text{SR}$, the beating degree of broad-leaved wood pulp is $35 \pm 1^\circ \text{SR}$, and the proportions of coniferous wood pulp are 50%, 60%, 70%, 80%, 90%, and 100% respectively. As shown in Figure 4, with the increase in the proportion of coniferous wood pulp, the average pores and maximum pores of the original medical dialysis paper gradually increase. The linear path function is used to process the images. Since the value of the linear path function

approaches 0 and tends to be stable after a pixel distance of 25, only the L2 values within the 0-25 pixel distance are considered.

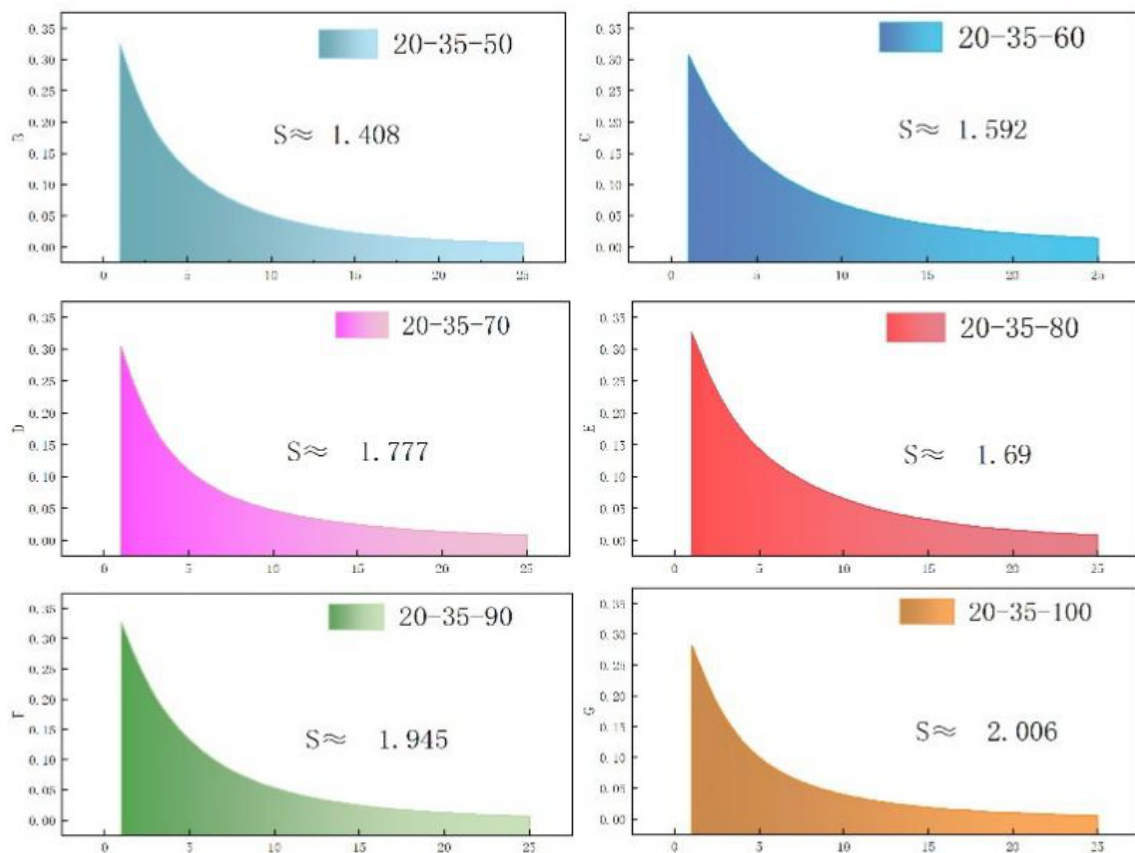


Fig. 4. L_2 Function and its integral value of the SEM images of the paper structure of the original medical dialysis paper under different proportions of coniferous wood pulp.

Figure 4 shows the L_2 function curves of the above SEM images within the pixel range of 0 to 25. The S values calculated according to Formula 2-3 indicate that with the increase in the coniferous wood content, the S values show an upward trend, indicating that the pore connectivity has been enhanced. This trend may be attributed to the unique structural characteristics of coniferous wood fibers. Coniferous wood fibers are usually longer and more flexible, which helps to form a more compact fiber network structure during the paper forming process, thereby improving the pore connectivity. In addition, a higher coniferous wood content may lead to an increase in the bonding force between fibers, further promoting the optimization of the pore structure. This finding is of great significance for optimizing the physical properties of paper, such as air permeability and mechanical strength. By adjusting the proportion of coniferous wood, the pore structure of paper can be effectively controlled to meet the requirements of different applications.

4.2.2. Regulation rules of coniferous wood beating degree on air permeability

In order to analyze the influence of the change in the beating degree of coniferous wood pulp on the properties of the original paper for medical dialysis, the data obtained from the experiment were analyzed. Figure 5 shows the influence of the beating degree of coniferous wood pulp on the air permeability of the original paper for medical dialysis.

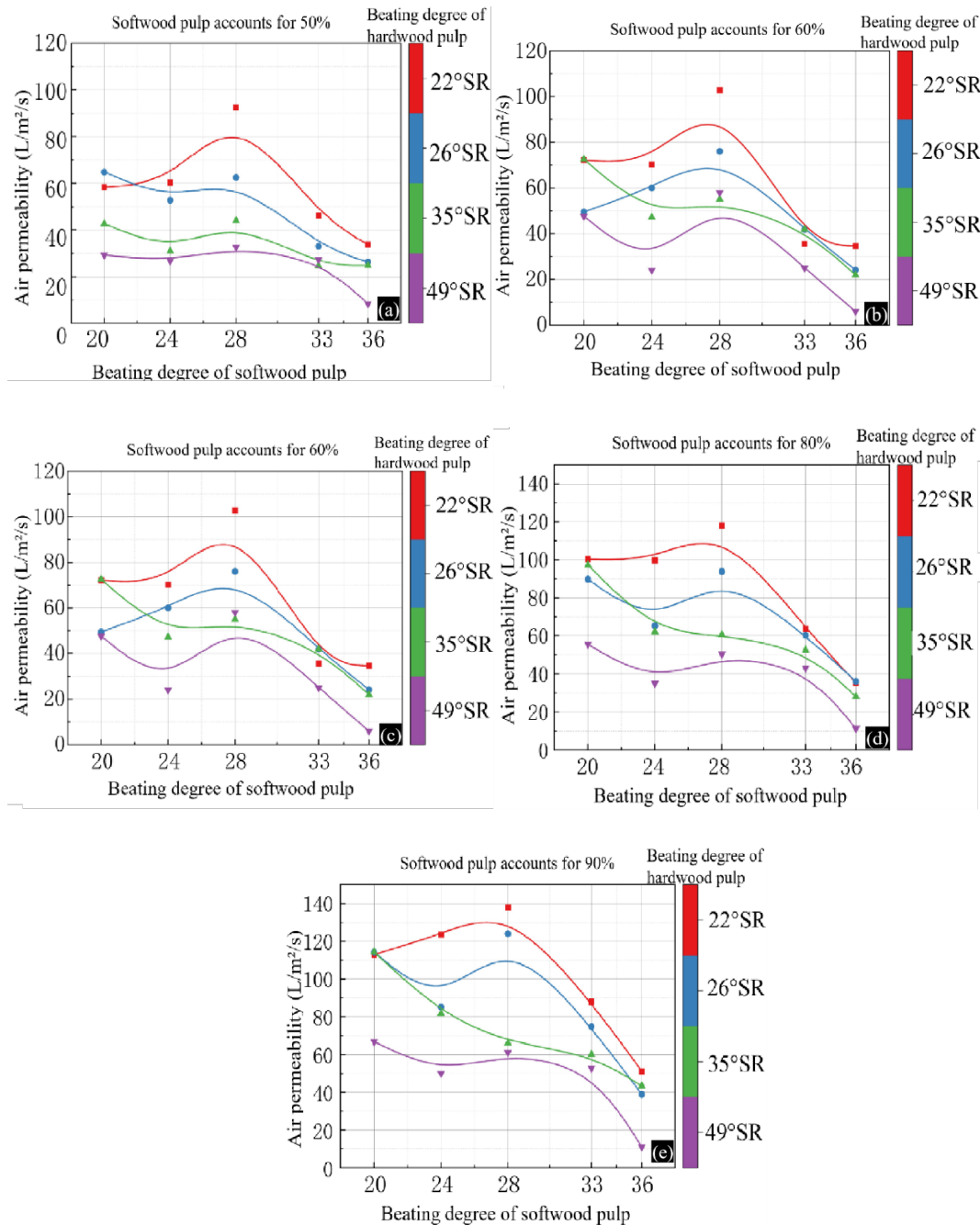


Fig. 5. The influence of the beating degree of coniferous wood pulp on the properties of the original medical dialysis paper under different proportions of coniferous wood.

As shown in Figure 5, there is a significant negative correlation between the beating degree of coniferous wood pulp and the air permeability of the original medical dialysis paper. Experimental data show that when the proportion of coniferous wood pulp is constant at 70% and the beating degree of broad-leaved wood pulp is $35 \pm 1^\circ\text{SR}$, as the beating degree of coniferous wood pulp increases from $20 \pm 1^\circ\text{SR}$ to $36 \pm 1^\circ\text{SR}$ in gradients, the air permeability of the original paper decreases successively from $78.98 \text{ L}/(\text{m}^2 \cdot \text{s})$ to $69.3 \text{ L}/(\text{m}^2 \cdot \text{s})$, $54.96 \text{ L}/(\text{m}^2 \cdot \text{s})$, $50.06 \text{ L}/(\text{m}^2 \cdot \text{s})$ and $32.18 \text{ L}/(\text{m}^2 \cdot \text{s})$, with a reduction range of 59.3%. This rule is universal in different beating degree systems of broad-leaved wood pulp ($22 \pm 1^\circ\text{SR}$, $36 \pm 1^\circ\text{SR}$, $49 \pm 1^\circ\text{SR}$), indicating that the beating process has a decisive regulatory effect on the pore structure of the fiber network.

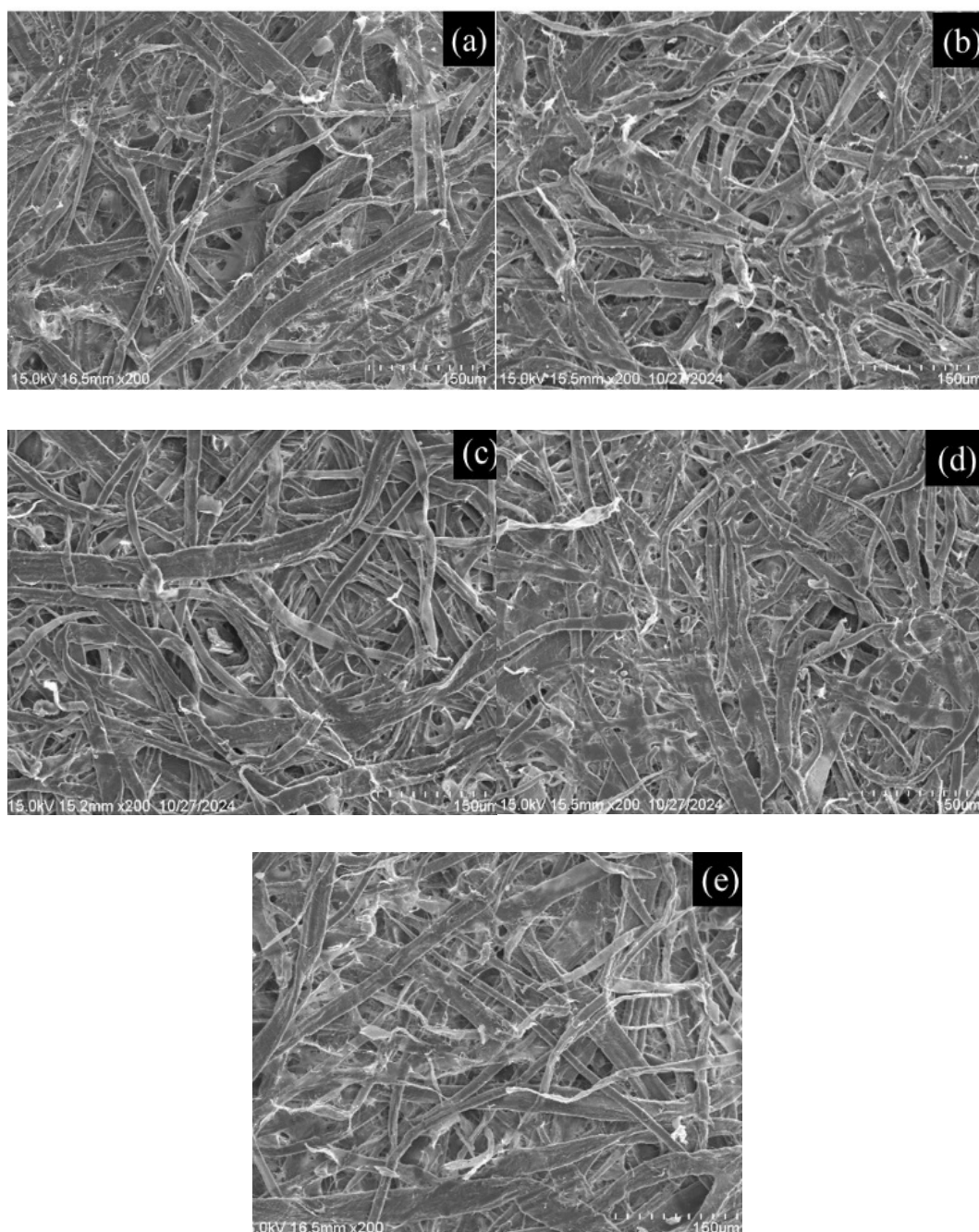


Fig. 6. SEM Images of the paper structure of the original medical dialysis paper under different beating degrees of coniferous wood pulp (a) $20 \pm 1^\circ\text{SR}$, (b) $24 \pm 1^\circ\text{SR}$, (c) $28 \pm 1^\circ\text{SR}$, (d) $33 \pm 1^\circ\text{SR}$, (e) $36 \pm 1^\circ\text{SR}$.

In order to analyze the influence of the change in the beating degree of coniferous wood pulp on the overall pore space of the original medical dialysis paper, Figure 6 shows the SEM images taken when the proportion of coniferous wood pulp is 70%, the beating degree of broad-leaved wood pulp is $35 \pm 1^\circ\text{SR}$, and the beating degrees of coniferous wood pulp are $20 \pm 1^\circ\text{SR}$, $24 \pm 1^\circ\text{SR}$, $28 \pm 1^\circ\text{SR}$, $33 \pm 1^\circ\text{SR}$ and $36 \pm 1^\circ\text{SR}$ respectively.

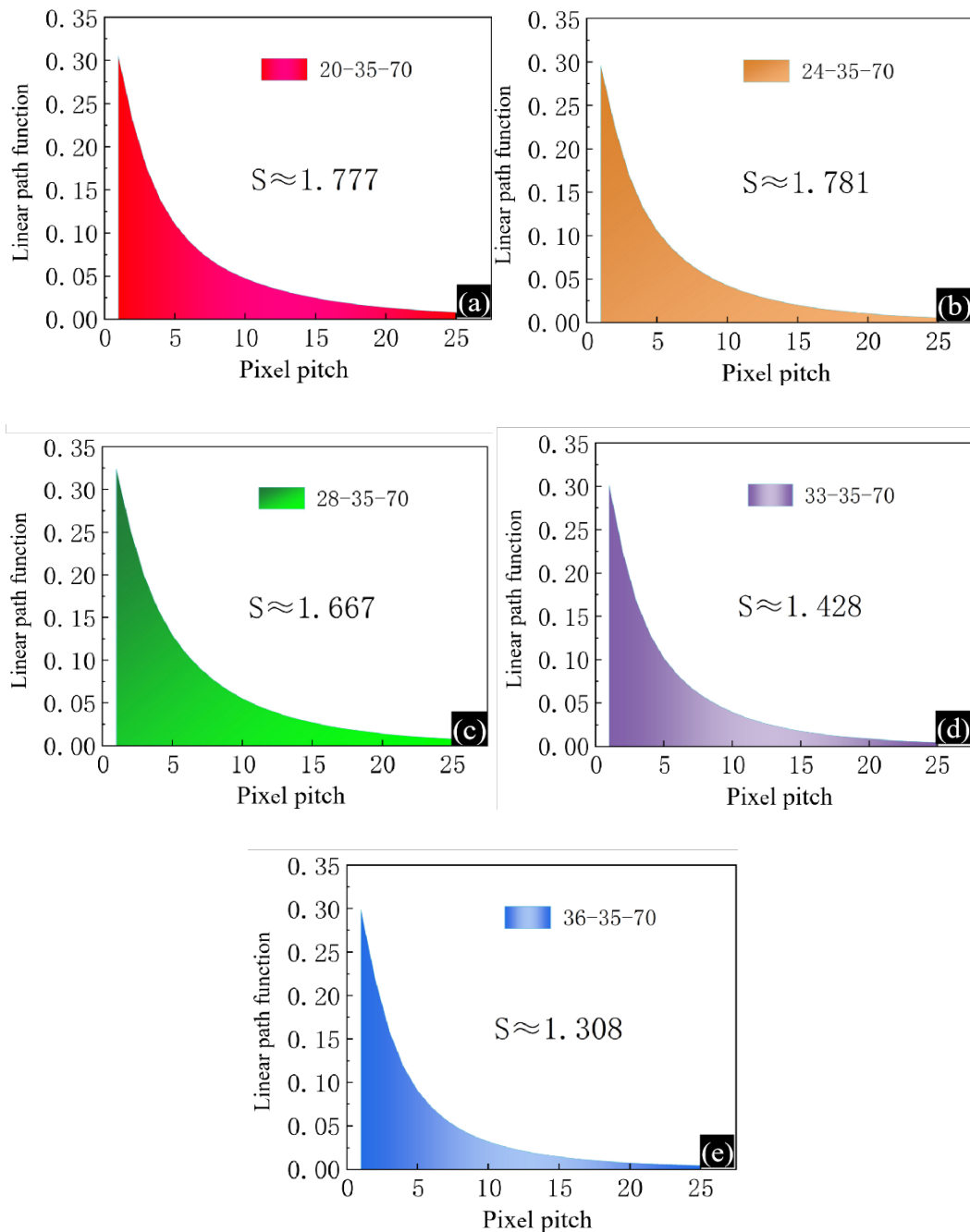


Fig. 7. L_2 Function images of the SEM images of the paper structure of the original medical dialysis paper under different beating degrees of coniferous wood pulp: (a) $20 \pm 1^\circ\text{SR}$; (b) $24 \pm 1^\circ\text{SR}$; (c) $28 \pm 1^\circ\text{SR}$; (d) $33 \pm 1^\circ\text{SR}$; (e) $36 \pm 1^\circ\text{SR}$.

Figure 7 shows the L_2 function curves of the above SEM images within the pixel range of 0 to 25. The S values calculated according to Formula 2-6 indicate that with the increase in the beating degree of coniferous wood pulp, the S values show a downward trend, indicating a weakening of pore connectivity. This trend may originate from the changes in the fiber structure during the beating process. As the beating degree increases, coniferous wood fibers gradually become finer, and the bonding force between fibers strengthens, resulting in a decrease in pore size and a reduction in pore connectivity. This phenomenon is closely related to the influence of the pore structure of wood on fluid migration, affecting the quality of processes such as drying, impregnation, and modification of wood. Therefore, controlling the beating degree is of great significance for adjusting the pore structure and properties of paper.

4.2.3. Regulation rules of broad-leaved wood beating degree on air permeability

In order to analyze the influence of the change in the beating degree of broad-leaved wood pulp on the properties of the original paper for medical dialysis, the data obtained from the experiment were analyzed. Figure 8 shows the influence of the beating degree of broad-leaved wood pulp on the air permeability of the original paper for medical dialysis.

As shown in Figure 8, with the increase in the beating degree of broad-leaved wood pulp, the air permeability of the original medical dialysis paper generally shows a downward trend. For example, when the proportion of coniferous wood pulp is 70%, the beating degree of coniferous wood pulp is $24 \pm 1^\circ\text{SR}$, and the beating degree of broad-leaved wood pulp is $22 \pm 1^\circ\text{SR}$, the air permeability of the original paper is $83.12 \text{ L}/(\text{m}^2 \cdot \text{s})$. As the beating degree of broad-leaved wood pulp increases to $26 \pm 1^\circ\text{SR}$, $35 \pm 1^\circ\text{SR}$, and $49 \pm 1^\circ\text{SR}$, the air permeability decreases to $72.56 \text{ L}/(\text{m}^2 \cdot \text{s})$, $69.3 \text{ L}/(\text{m}^2 \cdot \text{s})$, and $26.16 \text{ L}/(\text{m}^2 \cdot \text{s})$ respectively. Similarly, for broad-leaved wood pulps with beating degrees of $20 \pm 1^\circ\text{SR}$, $28 \pm 1^\circ\text{SR}$, $33 \pm 1^\circ\text{SR}$, and $36 \pm 1^\circ\text{SR}$, the overall trend also shows a downward trend. The main reason for this phenomenon may be the same as that of the influence of the beating degree of coniferous wood pulp on the air permeability of the original medical dialysis paper. However, its descending curve is steeper than that of the influence curve of the beating degree of coniferous wood pulp. This may be because coniferous wood pulp has higher toughness, while broad-leaved wood pulp fibers are relatively loose and more easily broken into fine fibers to fill the pores.

In order to analyze the influence of the change in the beating degree of broad-leaved wood pulp on the overall pore space of the original medical dialysis paper, Figure 9 shows the SEM images taken when the proportion of coniferous wood pulp is 70%, the beating degree of coniferous wood pulp is $24 \pm 1^\circ\text{SR}$, and the beating degrees of broad-leaved wood pulp are $22 \pm 1^\circ\text{SR}$, $26 \pm 1^\circ\text{SR}$, $35 \pm 1^\circ\text{SR}$ and $49 \pm 1^\circ\text{SR}$ respectively. As shown in Figure 2-8, with the increase in the beating degree of broad-leaved wood pulp, the average pores and maximum pores of the original medical dialysis paper gradually decrease.

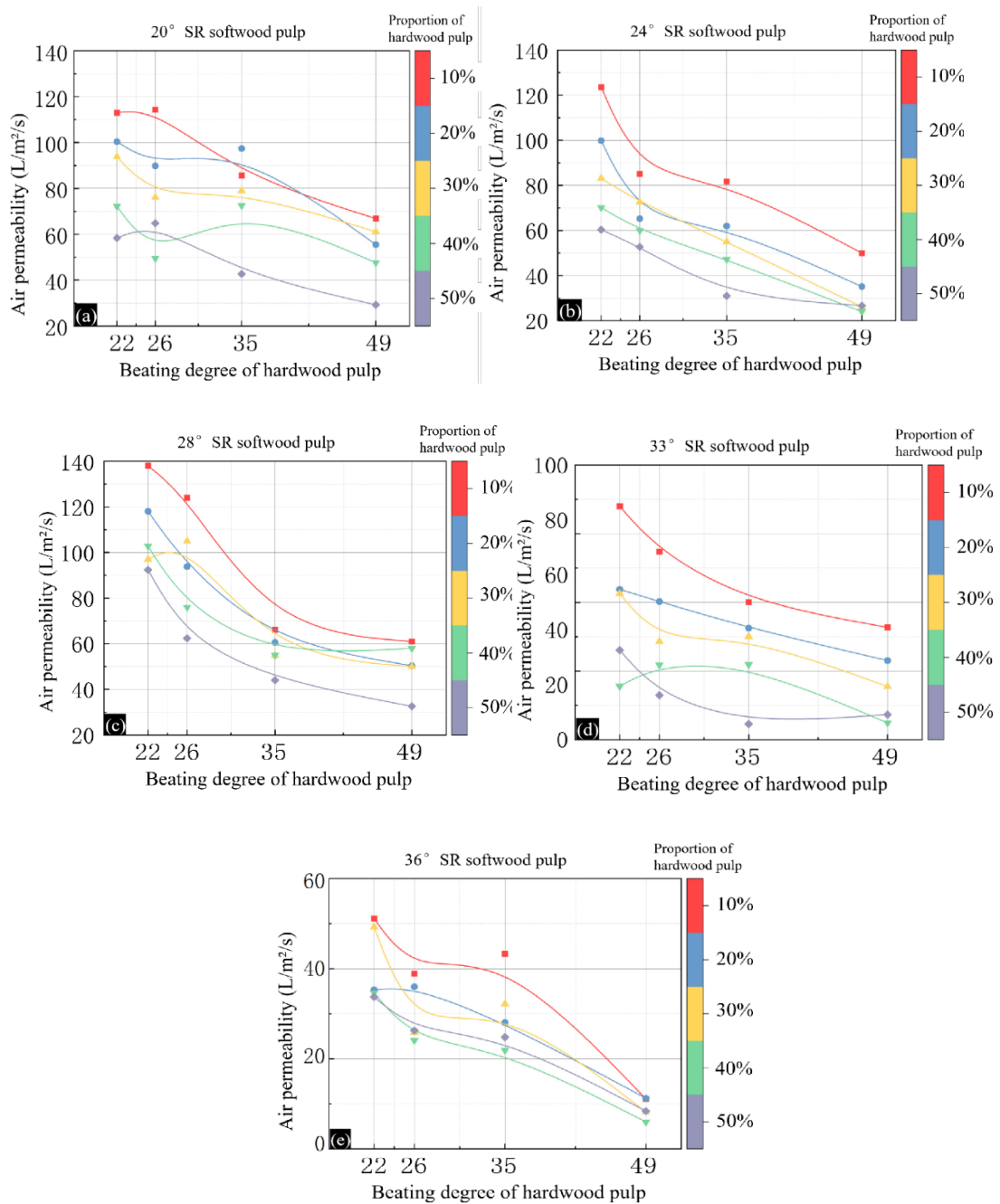


Fig. 8. The influence of different beating degrees of broad - leaved wood pulp on the air permeability of the original medical dialysis paper (a) Coniferous wood pulp at 20°SR; (b) Coniferous wood pulp at 24°SR; (c) Coniferous wood pulp at 28°SR; (d) Coniferous wood pulp at 33°SR; (e) Coniferous wood pulp at 36°SR.

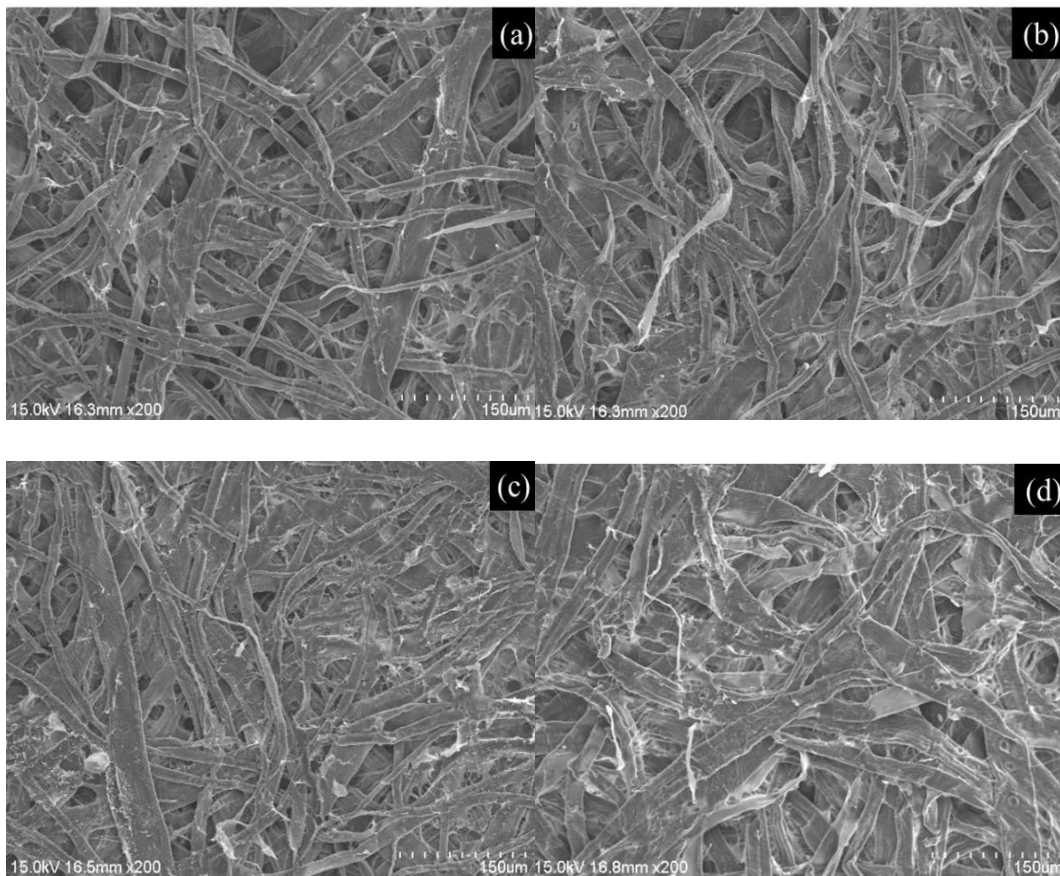


Fig. 9. SEM Images of the paper structure of the original medical dialysis paper under different beating degrees of broad - leaved wood pulp (a) $22\pm 1^\circ\text{SR}$, (b) $26\pm 1^\circ\text{SR}$, (c) $35\pm 1^\circ\text{SR}$, (d) $49\pm 1^\circ\text{SR}$.

Figure 10 shows the L_2 function curves of the above SEM images within the pixel range of 0 to 25. The S values calculated according to Formula 2-9 indicate that with the increase in the beating degree of broad-leaved wood pulp, the S values generally show a downward trend, indicating a weakening of pore connectivity. This phenomenon may be closely related to the structural characteristics of broad-leaved wood fibers and their changes during the beating process. Broad-leaved wood fibers are usually shorter and have thinner cell walls. During the beating process, they are more prone to being refined and broken, resulting in an increase in the bonding force between fibers and the formation of a denser fiber network structure. This densification may reduce the size and number of pores, thereby reducing the connectivity of pores.

In addition, changes in the pore structure have a direct impact on the physical properties of paper. The reduction in pore connectivity may lead to a decrease in the air permeability of the paper, but at the same time, it may improve its barrier properties and surface smoothness. Therefore, in the papermaking process, it is necessary to reasonably control the beating degree of coniferous wood pulp, the beating degree of broad-leaved wood pulp, and the proportion of coniferous wood pulp according to the performance requirements of the final product, so as to achieve an optimized balance between the pore structure and the paper properties.

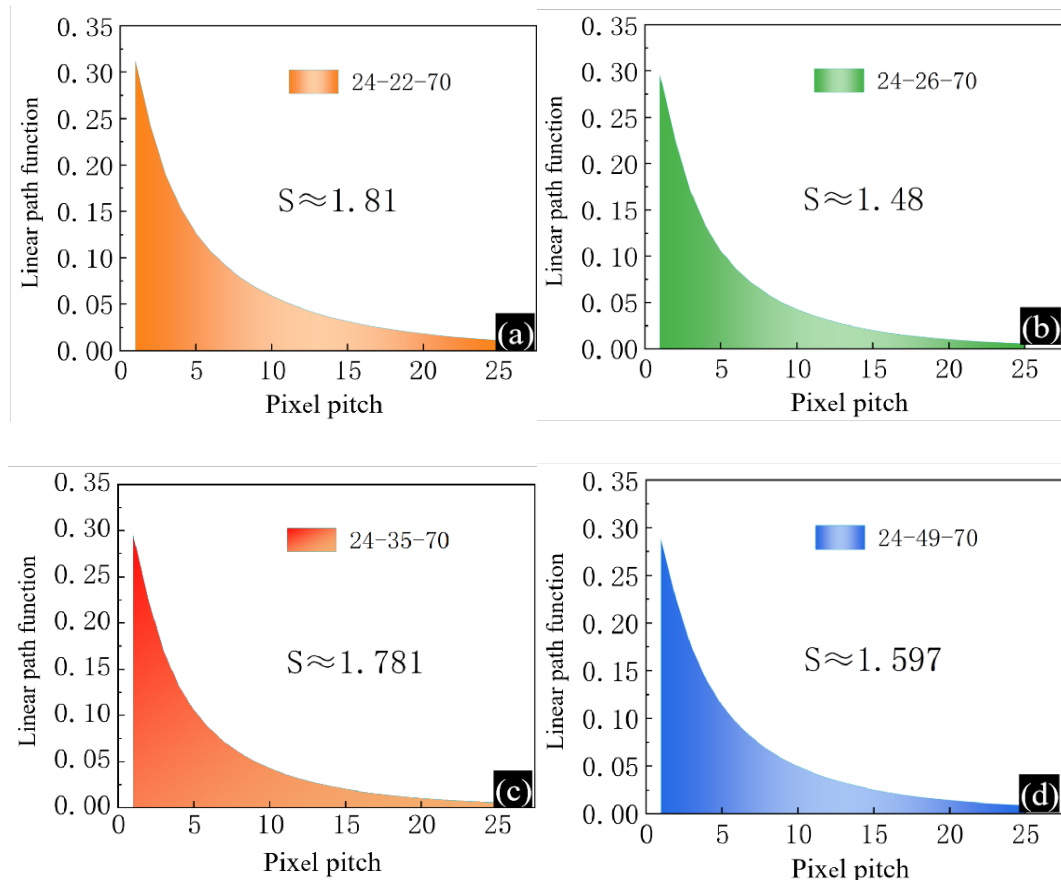


Fig. 10. L_2 Function images of the SEM images of the paper structure of the original medical dialysis paper under different beating degrees of coniferous wood pulp: (a) $22 \pm 1^\circ \text{SR}$; (b) $26 \pm 1^\circ \text{SR}$; (c) $35 \pm 1^\circ \text{SR}$; (d) $49 \pm 1^\circ \text{SR}$.

4.3. Regulation mechanism of pore size distribution

In this study, the pore structure of paper is usually characterized by two indicators: average pore size and most probable pore size[15]. Among them, the average pore size reflects the mean value of the entire pore size distribution, while the most probable pore size represents the pore size value that appears with the highest frequency in the pore size distribution.

Figure 11 shows the influence of the proportion of coniferous wood pulp on the pore size distribution of paper sheets under different beating degree conditions. Figures (a) to (e) respectively show the trends of the average pore size and the most probable pore size of the paper sheets with the change in the proportion of coniferous wood pulp at 20°SR , 24°SR , 28°SR , 33°SR and 36°SR . From the analysis of the change in the proportion of coniferous wood pulp, as the proportion of coniferous wood pulp increases, both the average pore size and the most probable pore size of the paper sheets show an upward trend. This phenomenon indicates that the proportion of coniferous wood pulp has a significant influence on the pore structure. When the beating degree is low, the bonding force of fibers is weak and the pore size distribution is relatively scattered. As the beating degree increases, the fineness and flexibility of fibers are enhanced, the bonding force between fibers is improved, the pore structure becomes more compact, and the amplitude of pore size growth decreases relatively.

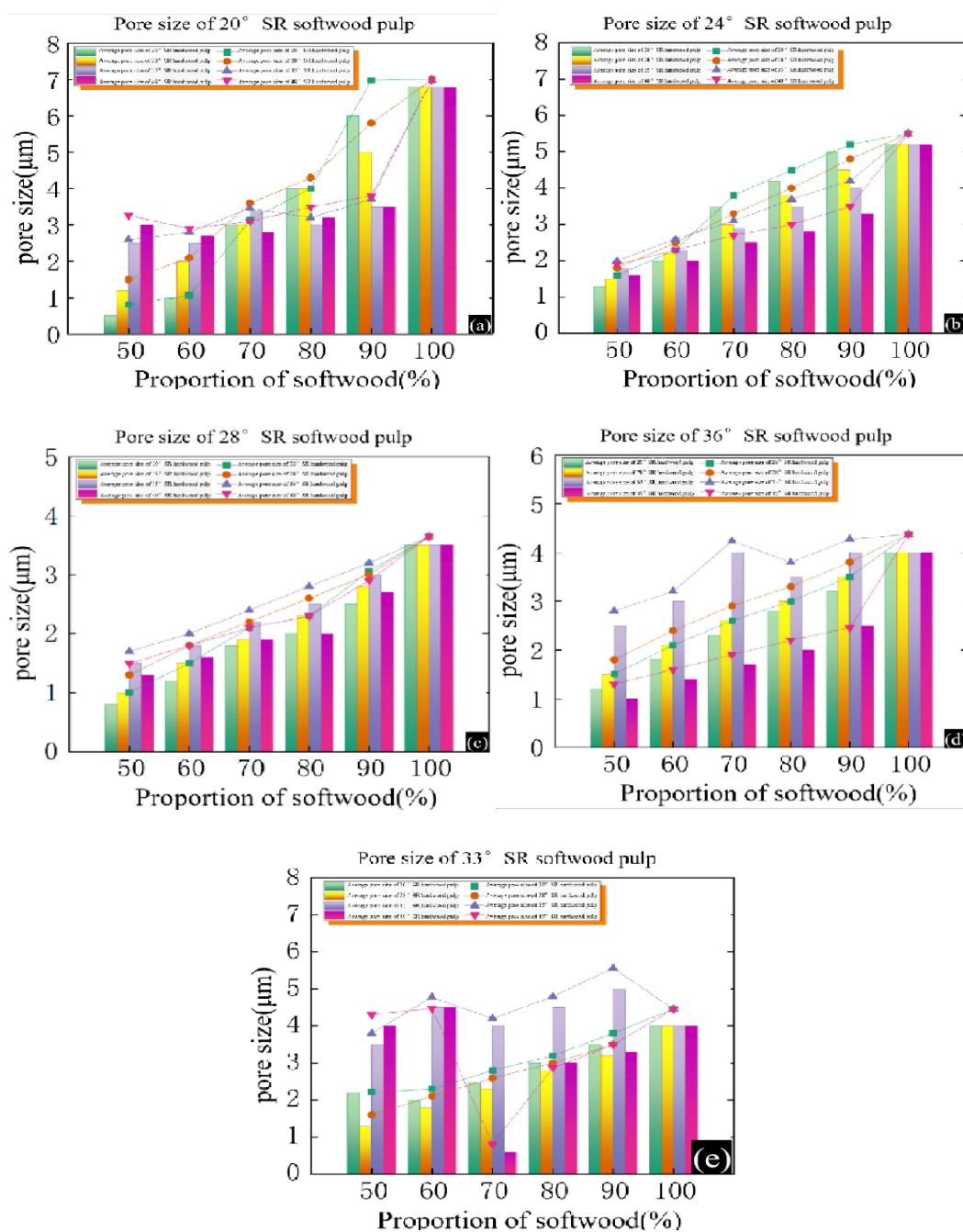


Fig. 11. The influence of different manufacturing parameters of the original medical dialysis paper on the average pore size and the most probable pore size. (a) Coniferous wood pulp at 20°SR; (b) Coniferous wood pulp at 24°SR; (c) Coniferous wood pulp at 28°SR; (d) Coniferous wood pulp at 33°SR; (e) Coniferous wood pulp at 36°SR.

From the analysis of the change in the beating degree of coniferous wood pulp, as the beating degree of coniferous wood pulp increases, the average pore size and the most probable pore size of the paper sheet generally show a downward trend. This indicates that during the beating process, coniferous wood fibers gradually become finer, the outer fiber walls rupture, and the number of fine fibers and microfibrils increases, thereby enhancing the bonding force between fibers and making

the paper sheet structure more compact. Especially at higher beating degrees, the cross-linking effect of coniferous wood fibers is enhanced, resulting in pore shrinkage and a more stable pore size distribution. However, at lower beating degrees, coniferous wood fibers are relatively rigid and the bonding force is weaker, resulting in larger pores and a relatively dispersed pore size distribution. This shows that the beating degree plays a key role in regulating the pore size structure of coniferous wood pulp.

From the analysis of the change in the beating degree of broad-leaved wood pulp, as the beating degree of broad-leaved wood pulp increases, the average pore size and the most probable pore size of the paper sheet first decrease and then tend to be stable. This is mainly because broad-leaved wood fibers are shorter and have thinner walls. During the beating process, their microfibrils are released earlier, resulting in a more significant filling effect between fibers, which rapidly reduces the pores. However, when the beating degree reaches a certain level, further beating makes it difficult to significantly change the fiber morphology, and the bonding force between fibers tends to be saturated, reducing the amplitude of pore structure changes. Therefore, the change in the beating degree of broad-leaved wood pulp has a greater impact on the pore structure in the early stage of regulation, and its influence gradually slows down at high beating degrees.

Further analysis of the specific trends under each beating degree reveals that under low beating degree conditions (20°SR and 24°SR), the pore size changes under different proportions of coniferous wood pulp are more pronounced, with a faster growth rate of the average pore size and the most probable pore size, indicating that the bonding between fibers is relatively weak and the pores are larger at this time. Under higher beating degree conditions (33°SR and 36°SR), the pore size change trend tends to be more stable, especially the growth amplitude of the most probable pore size decreases. This may be attributed to the enhanced fiber refinement and increased filling effect, which cause the pores to shrink and tend to be stable.

In addition, it can be observed from the curved parts of the figure that with the increase in the proportion of coniferous wood pulp, there are certain differences in the pore size distribution under different beating degrees. Among them, at beating degrees of 28°SR and above, when the proportion of coniferous wood pulp is relatively high ($>80\%$), the amplitude of pore size change tends to slow down, indicating that the densification degree of the fiber network has approached a stable state. Overall, these results indicate that by adjusting the proportion of coniferous wood pulp and the beating degree, the pore structure of the paper sheet can be effectively regulated, providing theoretical support for optimizing the air permeability and filtration performance of the paper.

A comparative analysis of the average pore size and the most probable pore size under different beating degrees and fiber blending conditions was conducted. The results show that under all experimental conditions, the trends of change of the two are highly consistent, and the numerical differences are relatively small. This indicates that within the scope of fiber structure and beating parameters involved in this study, the deviation between the most probable pore size and the average pore size is low. Using the average pore size as a characterization indicator can effectively represent the pore structure characteristics[15] without causing the loss of important information. In addition, the average pore size can provide more stable statistical results, which helps to reduce experimental errors and improve the comparability of data. Therefore, in the subsequent analysis of this study, the average pore size will be mainly used as the core parameter for characterizing the pore structure to ensure the scientificity and rationality of the analysis.

5. Conclusions

This study systematically reveals the regulation mechanisms of the proportion of coniferous wood pulp (50%-100%) and the beating degrees of coniferous and broad-leaved wood pulps (20-36°SR; 22-49°SR) on the air permeability, pore size distribution, and pore connectivity of the original medical dialysis paper. The experimental results show that the increase in the proportion of coniferous wood pulp significantly improves the air permeability (from 58.36 to 172.14 L/(m²·s)) through the three-dimensional network skeleton formed by its long fibers (number average length 1.0 - 1.3 mm, aspect ratio about 60:1), accompanied by an enhancement in pore connectivity (an increase of 62% in the S value). However, it is necessary to optimize the pore size distribution to control the maximum pore size to be less than 35 μm (for example, when the proportion of coniferous wood pulp is 80%, the maximum pore size is 34.7 μm) to meet the antibacterial requirements of ISO 11607.

The increase in the beating degree densifies the pore structure (the air permeability decreases by 59.3%-68.5%, and the average pore size decreases from 18.3 μm to 9.7 μm) by refining the fibers (the width of coniferous wood fibers decreases from 34.3 μm to 31.8 μm) and enhancing the bonding force between fibers through the release of microfibrils, while suppressing the dispersion of the pore size distribution (the standard deviation decreases from 4.2 μm to 1.8 μm). The study further verifies the predictive capabilities of the linear path function (L_2) and the integral S value model ($R^2 = 0.93$), confirming the strong correlation between process parameters and properties, and providing a theoretical framework for optimizing the synergistic effects of the proportion of coniferous wood pulp (70% - 80%) and the beating degree (24 - 28°SR) in industrial production.

Acknowledgments

The authors are thankful to the support of “Pioneer” and “Leading Goose” R&D Program of Zhejiang (Grant No. 2023C01195), the Natural Science Foundation of Zhejiang Province (Grant No. LTGS23C160001).

References

- [1] W. Gao, Z. Xiang, K. Chen, R. Yang, F. Yang, *Carbohydrate Polymers* 127 (2015) 400-406; <https://doi.org/10.1016/j.carbpol.2015.04.005>
- [2] G. Zhu, D. Kremenakova, Y. Wang, J. Militky, *Autex Research Journal* 15 (2015) 8-12; <https://doi.org/10.2478/aut-2014-0019>
- [3] X. Chen, S. Zhang, D. Hou, H. Duan, B. Deng, Z. Zeng, B. Liu, L. Sun, R. Song, J. Du, P. Gao, H. Peng, Z. Liu, L. Wang, *ACS Appl. Mater. Interfaces* 13 (2021) 29926-29935; <https://doi.org/10.1021/acsami.1c06243>
- [4] H. Aslannejad, S.M. Hassanizadeh, A. Raoof, D.A.M. De Winter, N. Tomozeiu, M.Th. Van Genuchten, *Chemical Engineering Science* 160 (2017) 275-280; <https://doi.org/10.1016/j.ces.2016.11.021>
- [5] X. Zhao, J. Yao, Y. Yi, *Transp Porous Med* 69 (2007) 1-11; <https://doi.org/10.1007/s11242->

[006-9052-9](#)

- [6] C. Knudby, J. Carrera, J.D. Bumgardner, G.E. Fogg, *Advances in Water Resources* 29 (2006) 590-604; <https://doi.org/10.1016/j.advwatres.2005.07.002>
- [7] J. Havelka, A. Kučerová, J. Sýkora, *Computational Materials Science* 122 (2016) 102-117; <https://doi.org/10.1016/j.commatsci.2016.04.044>
- [8] W.-J. Beyn, B. Gess, P. Lescot, M. Röckner, *Communications in Partial Differential Equations* 36 (2010) 446-469; <https://doi.org/10.1080/03605302.2010.523919>
- [9] P.T. Larsson, T. Lindström, L.A. Carlsson, C. Fellers, *J Mater Sci* 53 (2018) 3006-3015; <https://doi.org/10.1007/s10853-017-1683-4>
- [10] N.H. Vonk, M.G.D. Geers, J.P.M. Hoefnagels, *Nordic Pulp & Paper Research Journal* 36 (2021) 61-74; <https://doi.org/10.1515/npprj-2020-0071>
- [11] M. Alimadadi, S.B. Lindström, A. Kulachenko, *Soft Matter* 14 (2018) 8945-8955; <https://doi.org/10.1039/C7SM02561K>
- [12] Z. Jia, L.A. Campos, *IEEE Network* 35 (2021) 8-14; <https://doi.org/10.1109/MNET.011.2000612>
- [13] C. Burbano-Garcia, G. Araya-Letelier, R. Astroza, Y.F. Silva, *Construction and Building Materials* 343 (2022) 128102; <https://doi.org/10.1016/j.conbuildmat.2022.128102>
- [14] S. Mahade, A. Venkat, N. Curry, M. Leitner, S. Joshi, *Coatings* 11 (2021) 86; <https://doi.org/10.3390/coatings11010086>
- [15] P. Wang, J.B. Li, L. Zhou, K. Vafai, *Energy Conversion and Management* 212 (2020) 112795; <https://doi.org/10.1016/j.enconman.2020.112795>